Applied Catalysis B: Environmental 94 (2010) 311–317

Contents lists available at ScienceDirect

Applied Catalysis B: Environmental

journal homepage: www.elsevier.com/locate/apcatb

Low CO content hydrogen production from bio-ethanol using a combined plasma reforming–catalytic water gas shift reactor

Xinli Zhu, Trung Hoang, Lance L. Lobban, Richard G. Mallinson *

Center for Biomass Refining, School of Chemical, Biological, and Materials Engineering, The University of Oklahoma, Norman, OK 73019, USA

ARTICLE INFO

Article history:
Received 16 September 2009
Received in revised form 30 November 2009
Accepted 3 December 2009
Available online 16 December 2009

Keywords:
Hydrogen production
Plasma
Ethanol reforming
Water gas shift
Pt–Re/TiO_2

ABSTRACT

Bio-ethanol reforming was studied using a plasma-catalytic reactor for hydrogen production at low temperature and atmospheric pressure without diluent gas or external heating. The plasma applied was a DC pulse discharge (corona) plasma. The water gas shift (WGS) catalyst was put just below the cathode electrode. The discharge generated heat was effectively used for feed vaporization and the WGS reaction. The large amounts of CO (~30%) in the H_2 rich gas formed in plasma reforming of ethanol (H_2O/ethanol = 6) was successfully reduced to ~0.8% when a Pt/TiO_2 and Pt–Re/TiO_2 stacked bed were used for in situ WGS catalysis with a gas hourly space velocity up to 12,000 $cm^3\ g^{-1}\ h^{-1}$. The resultant gases contain ~73% H_2 and ~23% CO_2, with small amounts of CO, CH_4, and C_2H_6, that is suitable for H_2 fuel cell use after residual CO removal. Stability tests with daily startup–shutdown showed both plasma and catalyst are stable. The plasma-catalytic system is promising for low CO content H_2 production, and could be extended to other applications.

1. Introduction

Hydrogen fuel cells receive growing attention because they theoretically have a higher energy efficiency than internal combustion engines and no direct greenhouse gas emissions, and also have potential applications for small scale power generation, for example, mobile and distributed power stations. Hydrogen production for fuel cells is one of the key issues for successful commercial development of fuel cell technology [1,2]. Due to the lack of existing transportation infrastructure and effective storage technology for H_2, large scale industrially produced H_2 cannot be easily used for distributed and mobile fuel cell applications. Onboard (or distributed small scale production for this and other small scale power applications) H_2 production thus has been recognized as an alternative. Bio-ethanol is a good candidate for H_2 production for fuel cells because it is non-toxic, renewable, and easy for transportation and storage [3]. Ethanol for this purpose also, does not requires complete removal of water, thus lowering the cost of ethanol production, once this application becomes widespread.

Since hydrogen for fuel cells requires ultra low CO concentration (<50 ppm) H_2, the system for H_2 production from bio-ethanol usually contains several consecutive reactors operated at different conditions: reforming of ethanol (EtOH), water gas shift (WGS), and CO preferential oxidation. Steam reforming of ethanol (1) is a strongly endothermic reaction that is thermodynamically favored at high temperatures. For a catalytic process, lowering the reaction temperature would result in side reactions producing large amounts of undesirable methane, acetaldehyde, and ethylene, that will lower the final hydrogen yield [4–6]. Thus, high reaction temperatures of ~700 °C are needed to maximize the H_2 yield and minimize the side reactions [4]. The WGS reaction (2) is not suited to operate at similar conditions, since high CO conversion is thermodynamically favored at low temperatures. A second reactor operated at lower temperatures (200–400 °C) for the WGS reaction is necessary to convert CO to additional H_2. The WGS reaction rate is strongly limited by kinetics at low temperature [7,8]. Therefore, active and stable catalysts with high reaction rates are highly desirable in order to minimize the overall reactor volume and catalyst required [9,10]. In the last step, the residual CO may be removed to ppm level by CO preferential oxidation. If the reforming reaction (1) and WGS reaction (2) could be integrated to the net reaction (3) in a single reactor, the response time, compactness and energy integration of the system may be improved significantly.

$$C_2H_5OH + H_2O \rightarrow 2CO + 4H_2, \quad \Delta H = 256\ kJ/mol \tag{1}$$

$$CO + H_2O \rightarrow CO_2 + H_2, \quad \Delta H = -41\ kJ/mol \tag{2}$$

$$C_2H_5OH + 3H_2O \rightarrow 2CO_2 + 6H_2, \quad \Delta H = 174\ kJ/mol \tag{3}$$

* Corresponding author at: Center for Biomass Refining, School of Chemical, Biological, and Materials Engineering, The University of Oklahoma, 100 E. Boyd Street, Room T335, Norman, OK 73019, USA. Fax: +1 405 325 5813.
E-mail address: mallinson@ou.edu (R.G. Mallinson).

0926-3373/$ – see front matter © 2009 Elsevier B.V. All rights reserved.
doi:10.1016/j.apcatb.2009.12.004

There are several drawbacks of a catalytic process for H_2 production from bio-ethanol. Steam reforming of EtOH operated at high temperature is an energy intensive process, resulting in high cost and lower efficiency for small scale operation. Furthermore, it is difficult to control and stabilize all the operational parameters for three (if single stage WGS is used) or four catalytic reactors (if high- and low temperature WGS are used) coupled in series [11]. The startup, shutdown, and transient operation responses are also relatively slow. In addition, the catalysts may suffer from deactivation due to coke formation, impurities, as well as sintering.

Non-equilibrium plasmas are a type of plasma characterized by very high electron temperature ($\sim 10^5$ K) while having a low bulk gas phase temperature (from room temperature to $<10^3$ K) [12,13]. The plasma may be initiated in a very short time in an atmospheric pressure gas by applying high voltage electricity [12,13]. The high energy and abundant electrons in the plasma activate reactants and initiate radical reactions. The plasma reaction has the advantages of low temperature, quick startup and shutdown, and free of catalyst deactivation. The literature shows exploitation of plasma reforming of hydrocarbons and oxygenated hydrocarbons, for example, CH_4 and EtOH, for H_2 production [14–26]. The major products in plasma steam reforming are H_2 and CO, accompanied by small amounts of CO_2 and hydrocarbons. The WGS reaction only takes place to a limited extent even with a large excess of water and at low reaction temperatures, largely being the result of the non-equilibrium properties of the plasma.

Although the non-equilibrium plasma is generated at room temperature, the temperature of the plasma may be up to several hundred degrees due to the collision energy transferred from the high energy electrons to stable molecules. In previous work of ours and others, it was observed that the temperature of surface wave discharge [18] and pulse corona discharge [26,27] plasmas could be in the range of 200–400 °C, which is a suitable temperature range for WGS reaction. In this work, plasma reforming and the catalytic WGS reaction have been integrated within one reactor and tested for bio-ethanol reforming. With proper plasma-catalytic reactor design and catalyst, the heat produced in the plasma is effectively used to vaporize the feed and also to drive the catalytic WGS reaction. The results show that H_2 with low CO concentration (<1%) is successfully produced without external heating using this integrated configuration.

2. Experimental

2.1. Configuration of plasma and plasma-catalytic reactors

Fig. 1 shows the plasma-catalytic reactor configuration, which has been described in previous work [26]. The reactor configuration is point to plate, with a discharge gap of 15 mm. The anode is made of stainless steel tubes, with a 1/16 in. o.d. tube inside of a 1/8 in. o.d. tube (these simply act as reducers). A hollow needle with an inner diameter of 0.26 mm is put inside the 1/16 in. tube close to the tip of the tube electrode. The cathode is made of 3/8 in. o.d. stainless steel tube with a 1/2 in. o.d. stainless steel sintered filter cap (~90 μm) on the top. The porous structure of the filter cap distributes the plasma homogeneously on the cathode and allows the vapor to pass through the filter which also ensures that all of the vapor passes through the plasma zone. The reactor vessel is a 1 in. o.d. quartz tube. The mixture of EtOH/H_2O is fed through the anode, and is vaporized inside of the tip of the anode before entering the plasma reaction zone for reaction. The products and unreacted reactants pass through the filter cap, exiting the reactor through the cathode. No diluent gases are used.

Infrared temperature measurement from outside of the reactor showed that the tip of the anode is the hottest point (~290 °C) of the plasma reactor, followed by the plasma zone (~260 °C) and the plate electrode (220–250 °C). The temperature drops quickly to ~160 °C for the anode 2 cm higher than the tip, and to ~110 °C for the cathode 2 cm lower than the filter cap. Therefore, the plasma heating effect is a localized phenomenon. Due to the low IR transparency of quartz, the true temperatures could be somewhat higher than these values, but this range has been validated in other studies [27]. This design allows the heat produced by the plasma on the anode to be quickly transferred to the liquid feed when it flows through the needle, thereby vaporizing the feed before entering the plasma zone. This configuration of the plasma reactor has several advantages [26]: (1) no external heating is needed; (2) easily combined with catalysts; (3) relatively smaller diameter of the cathode avoids discharge to the reactor wall, thus increasing the stability of the plasma; (4) all reactants are forced to pass through the discharge zone without bypassing; (5) erosion of the anode is reduced due to liquid cooling and (6) scalability that has also been demonstrated.

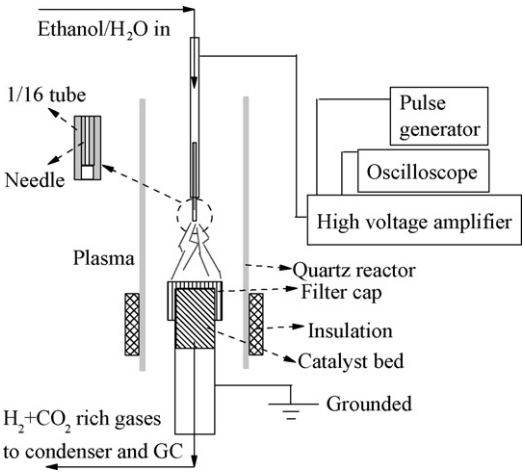

Fig. 1. Schematic representation of the plasma-catalytic reactor.

The WGS catalyst is put just below the filter cap and inside of the 3/8 in. tube of the cathode. If necessary, the catalyst zone is insulated from the outside of the reactor. Thus the temperature close to the top of the cathode is about ~300 °C (measured using a thermocouple from the outside of the reactor immediately after plasma was stopped). This temperature is suitable for a single stage WGS reactor.

2.2. Plasma and plasma-catalytic reaction

The plasma applied in this work is a DC pulse discharge (corona) plasma. The waveform was generated by a pulse generator (HP 8011A), and magnified by a high voltage amplifier (Trek, 20/20C). The discharge was monitored by an oscilloscope (Lecroy, wave surfer 422). The discharge current was set at 2 mA, and the pulse rate was 4000 pulse per second (pps). The discharge voltage was ~4.5 kV, and the power input was ~15 W.

EtOH/H_2O mixtures containing 30, 35, 40, 45, 50 vol.% EtOH, corresponding to H_2O/EtOH molar ratios of 7.56, 6.02, 4.86, 3.96, 3.24 were fed to the reactor using an HPLC pump once the plasma was initiated. The effluent product gas was analyzed by an online AGC 400 gas chromatograph (GC, Carle) after passing through an ice-water trap. The GC is equipped with a thermal conductivity detector (TCD), five columns and an HTS hydrogen transfer analysis system, that is capable of separating permanent gases (H_2, CO_2, CO, N_2, O_2) and hydrocarbons (up to C6). The condensed liquid was analyzed using a QP2010s GC–MS (Shimadzu), equipped with an Innowax capillary column. The major component of the liquid is

H_2O with small amounts of unreacted ethanol and trace amounts of acetaldehyde and acetone.

EtOH conversion to gas phase products (%) is defined as 100 × (total carbons in the gas phase products/total carbons in feed). Gaseous carbonaceous species (or H_2) selectivities (%) are defined as 100 × (carbons in species i (or H in H_2)/total carbons (or H) in converted ethanol to gas phase). With this definition, the maximum possible H_2 selectivity is 133.3% if the reaction follows only reaction (1) or 200% for the combined reaction (3).

2.3. Catalyst preparation, characterization, and catalytic water gas shift activity

The catalysts (1 wt% Pt/CeO_2, 1 wt% Pt/TiO_2, 1 wt% $Pt–Re/TiO_2$) used in this work were prepared by the incipient wetness impregnation method [28]. The CeO_2 was prepared by a precipitation method, and the TiO_2 was commercial Degussa P25 [28]. Briefly, after impregnation of the support with metal precursor at room temperature for 12 h, the resultant sample was dried at 100 °C for 12 h and then was calcined in flowing air at 400 °C for 4 h [28]. The dispersion of Pt was determined by chemisorption of CO. The catalyst sample (50 mg, 40–60 mesh) was reduced in flowing H_2 at 300 °C for 1 h, followed by He purging for 0.5 h to desorb H_2. Then the temperature was lowered to room temperature in flowing He. 100 μL of 5% CO/He was pulsed to the sample until a constant CO signal was obtained. The CO signal was monitored by a TCD using He as the reference gas. The Pt dispersion was calculated assuming a stoichiometric CO/Pt ratio of 1. The metal support interaction was studied by H_2 temperature programmed reduction (TPR). Catalyst samples (200 mg, 40–60 mesh) were subjected to flow by 5% H_2/Ar at room temperature for 3 h to stabilize the TCD signal. After that, the temperature was ramped to 900 °C with a rate of 10 °C/min. The H_2 consumption was monitored by a TCD.

The catalytic activity alone was evaluated under both differential reaction conditions (lower conversion) and simulated post-plasma reaction conditions (high CO concentration), using a 1/4 in. o.d. quartz reactor at atmospheric pressure. The catalyst sample (40–60 mesh) was reduced at 300 °C in flowing H_2 before shifting to reactant gases at the desired reaction temperature. For differential reaction conditions, the gas components were 3% CO–57% He–40% H_2, with a H_2O/CO of 2. The gas flow rate was varied from 30 cm^3/min to 500 cm^3/min, and the catalyst (20–100 mg) was mixed with α-Al_2O_3 to get a total weight of 100 mg. These conditions allowed the CO conversion to be kept to less than 10%. For the post-plasma simulated conditions, the gas components were 30% CO–70% H_2, with a H_2O/CO of 5, and have been described elsewhere [28]. The gases after reaction were analyzed using the online GC (Carle AGC 400). It should be noted that no hydrocarbon was detected either under differential reaction conditions or simulated post-plasma condition up to the maximum temperature tested, i.e. 350 °C.

3. Results and discussion

3.1. Catalyst characterizations and catalytic water gas shift reaction

Fig. 2 shows the H_2-TPR profiles of Pt/CeO_2, Pt/TiO_2, and $Pt–Re/TiO_2$. For Pt/CeO_2, the major peak centered at 292 °C and a wide peak >620 °C are observed, that can be assigned to reductions of PtO_2 plus surface ceria close to Pt and bulk ceria, respectively [29]. For Pt/TiO_2, two small peaks centered at 109 °C and 364 °C are related to Pt oxide species (PtO and/or PtO_2) and TiO_2, respectively [30]. The Pt species reduction temperature on TiO_2 is lower than that in the Pt/CeO_2, suggesting a relatively weak interaction of Pt-TiO_2 compared to that of Pt-CeO_2. For the $Pt–Re/TiO_2$ catalyst, a

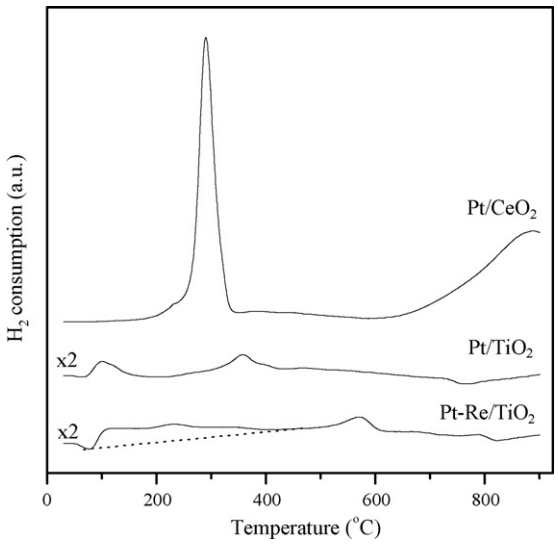

Fig. 2. H_2-TPR profiles of Pt/CeO_2, Pt/TiO_2, and $Pt–Re/TiO_2$.

weak and broad peak (from ca. 90 °C to ca. 400 °C) centered at 121 °C and a peak at 580 °C are present. The former can be ascribed to Pt and Re species, and the latter could result from TiO_2. The overlapping feature of the reduction of Pt and Re species indicates that Pt and Re species are interacting with each other. Thus, the Re species may stabilize the Pt particles from sintering. The relatively higher reduction temperature of TiO_2 in $Pt–Re/TiO_2$ than that in Pt/TiO_2 might result from the preferential interaction of Pt with Re in $Pt–Re/TiO_2$ while Pt is directly interacting with TiO_2 in the absence of Re. As a consequence, the hydrogen spillover from Pt to TiO_2 might be easier for Pt/TiO_2 thus resulting in a lower reduction temperature.

Table 1 summarizes the results for Pt dispersion, reaction rate and turnover frequency (TOF) for Pt/CeO_2, Pt/TiO_2, and $Pt–Re/TiO_2$ for the WGS reaction. Pt/CeO_2 has a Pt dispersion of 42.1%. However, when the sample was reduced at 200 °C, the dispersion was 58.1%. This difference can be explained by the Pt particle surface being partially covered by CeO_x species when it was reduced at 300 °C, as evidenced by the TPR results. The Pt dispersion is higher for the Re promoted sample than for the Pt only sample, which is in good agreement with the TEM results [28]. It should be noted that Re does not adsorb CO under the present conditions [31]. The WGS reaction rate is higher over the $Pt–Re/TiO_2$ than Pt/TiO_2 and higher than Pt/CeO_2 at 300 °C under differential reaction conditions. The Pt/TiO_2 and $Pt–Re/TiO_2$ have a similar TOF, indicating that the role of Re is to promote the Pt dispersion under these conditions. For the simulated post-plasma conditions, the reaction activity follows $Pt–Re/TiO_2 > Pt/CeO_2 > Pt/TiO_2$ [28].

Table 1
Pt dispersion, reaction rate and turnover frequency for WGS reaction over Pt/CeO_2, Pt/TiO_2, and $Pt–Re/TiO_2$ catalysts.

Samples	Pt dispersion (%)	Reaction rate[a] ($\times 10^{-6}$ mol g^{-1} s^{-1})	TOF[a] (s^{-1})
Pt/CeO_2	42.1	4.66	0.527
Pt/TiO_2	38.8	6.98	0.355
$Pt–Re/TiO_2$	60.7	10.83	0.351

[a] Measured at 300 °C under differential reaction conditions with CO conversion lower than 10%. Reaction rate is defined as moles of converted CO per gram catalyst per second; turn over frequency (TOF) is defined as molecules of converted CO per surface Pt atom per second.

Table 2
Effect of catalyst on EtOH conversion to gas phase products, H_2 production rate and selectivities to gas phase products of plasma-catalytic EtOH conversion.

Sample	Con.[a] (%)	H_2 production rate (mmol/min)	Gas phase composition (%)					
			H_2	CO_2	C_2H_4	C_2H_6	CH_4	CO
No catalyst	99	2.50	63.9	5.0	0.6	0.3	0.4	30.0
Pt/CeO_2 [b]	91	3.14	72.5	22.8	0	1.2	1.3	2.2
Pt/TiO_2 [c]	94	3.34	73.5	19.8	0	1.0	0.6	5.0
$Pt–Re/TiO_2$ [d]	94	3.44	72.6	21.6	0	1.2	1.1	3.5
$Pt/TiO_2 + Pt–Re/TiO_2$ [e]	97	3.56	73.3	23.6	0	1.4	0.9	0.8

Reaction conditions: 35 vol.% EtOH, 0.1 ml/min, catalyst bed zone insulated, 4.5 kV, 4 kpps, 2 mA.
[a] EtOH conversion to gas phase products.
[b] 1 g catalyst (dry gas based GHSV is ~6000 $cm^3 g^{-1} h^{-1}$), average of 1 h reaction.
[c] 1 g catalyst (dry gas based GHSV is ~6000 $cm^3 g^{-1} h^{-1}$), average of 1.5 h reaction.
[d] 0.6 g catalyst (dry gas based GHSV is ~10,000 $cm^3 g^{-1} h^{-1}$), average of 4 days run (about 26 h), includes daily start–stop, the catalyst sample was exposed to air when the reaction was stopped.
[e] 0.4 g Pt/TiO_2 followed by 0.6 g $Pt–Re/TiO_2$ (dry gas based GHSV is ~6000 $cm^3 g^{-1} h^{-1}$), average of 5 h run.

3.2. Plasma reforming of ethanol

The plasma used in this work is a high pulse rate discharge (corona) plasma, which has been suggested to have a higher efficiency than microwave discharges and silent discharges for CH_4 conversion [16]. The input pulse rate is determined by the current setting. A higher discharge current leads to a higher pulse rate and higher power input, leading to higher EtOH conversion rates. In this work, the current was set at 2 mA, resulting in a pulse rate of 4000 pulses per second (pps). The gas phase products of plasma reforming of EtOH are H_2, CO, CO_2, CH_4, C_2H_2, C_2H_4, and C_2H_6. Higher H_2O/EtOH ratios reduce the hydrocarbon selectivity and improve the WGS reaction, thus leading to higher H_2 yields, but less ethanol throughput and hydrogen production (molar rate). Table 2 reports the typical products distribution of 35 vol.% EtOH reforming. It can be seen that H_2 (63.9%) and CO (30%) are the main products, accompanied by small amounts of CO_2, CH_4, C_2H_4, and C_2H_6, indicating that the major reaction is reaction (1) and little WGS is observed. Note that C_2H_2 is not present under these conditions. Other plasma configurations and waveform inputs give similar products distributions, which are discussed elsewhere [32]. These results are in good agreement with the literature, showing that the plasma is unable to convert CO effectively to CO_2 and H_2 [15,17–19]. The high concentration of CO needs substantial reduction for H_2 fuel cell applications. It should be noted that the small amounts of C_2H_2 and C_2H_4 that might be formed would also need to be removed because they are easily adsorbed on the Pt electrode of fuel cells at low temperature.

3.3. Combined plasma reforming and catalytic water gas shift reaction

For the combined plasma reforming with catalytic WGS reaction, the catalyst was placed just below the cathode electrode. No pre-reduction was carried out. Therefore, the catalyst was reduced by the generated H_2 produced from the plasma reforming reaction. The catalyst reduction was usually complete within 15 min for first time use.

The catalyst bed was first tested using the Pt/TiO_2 catalyst. The selectivities of the gas phase products are plotted in Fig. 3. The Pt/CeO_2 result is also included as a reference, since it is a well known WGS catalyst. 1 g of catalyst was used for both Pt/TiO_2 and Pt/CeO_2, resulting in a gas hourly space velocity (GHSV) for WGS of ~6000 $cm^3 g^{-1} h^{-1}$ (based on dry gas). The H_2 selectivity is improved from 115.3% with no catalyst to 153.3% when Pt/TiO_2 was used as a catalyst without reactor insulation, and further improved to 177.9% when the catalyst bed zone was wrapped with insulation. At the same time, CO_2 selectivity increases (from 13.4% to 43.3% and 72.0%) whereas CO selectivity decreases (from 81.1% to 46.2% and 18.2%), these values are without catalyst, with catalyst and uninsulated, and with catalyst and insulated, respectively. The CO concentration was reduced to 5.0% for Pt/TiO_2 with insulation, as shown in Table 2. These results indicate that the WGS reaction occurs when the plasma product gases pass through the catalyst bed. Insulation of the catalyst bed keeps the catalyst bed hotter allowing the WGS reaction to take place at a higher reaction rate, but low enough to achieve a relatively low CO concentration. Therefore, there is a compromise to maintain a good reaction rate, but low equilibrium CO that can be achieved without external controls when the system is operated closer to adiabatically. It is not feasible to measure the temperature directly under these conditions because the discharge will disturb any thermocouple signal and instrumentation.

For the hydrocarbon products, only CH_4 and C_2H_6 are present when the catalyst was used irrespective of the presence or absence of insulation, implying the occurrence of hydrogenation of C_2H_4 to C_2H_6. The hydrogenations of C_2H_2 and C_2H_4 are readily completed over supported Pt, Pd catalysts at very low temperature [25,33,34]. Thus it is expected that hydrogenation readily takes place. Note that both CH_4 and C_2H_6 are inert for purposes of considering the effect on the Pt electrode of fuel cells at low temperature. The total hydrocarbon selectivities are increased when the catalyst was used. Because there are no hydrocarbons observed when using

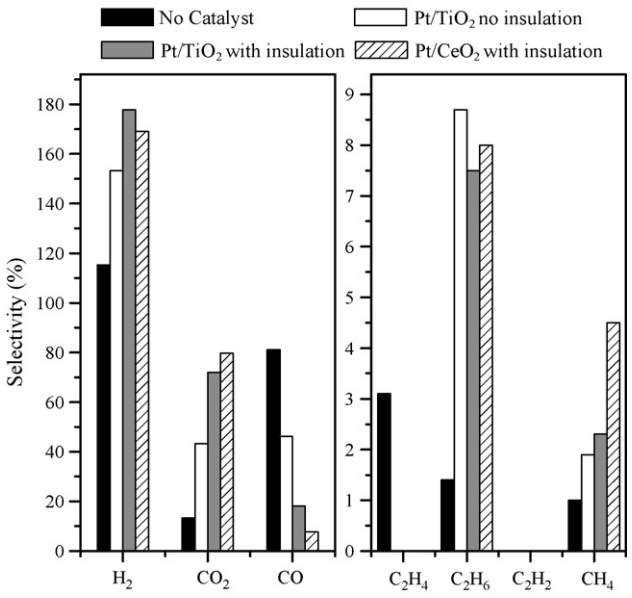

Fig. 3. Effect of catalyst and insulation on gas phase products selectivities of plasma-catalytic EtOH conversion. Reaction conditions: 35 vol% EtOH, 0.1 mL/min, 1 g catalyst.

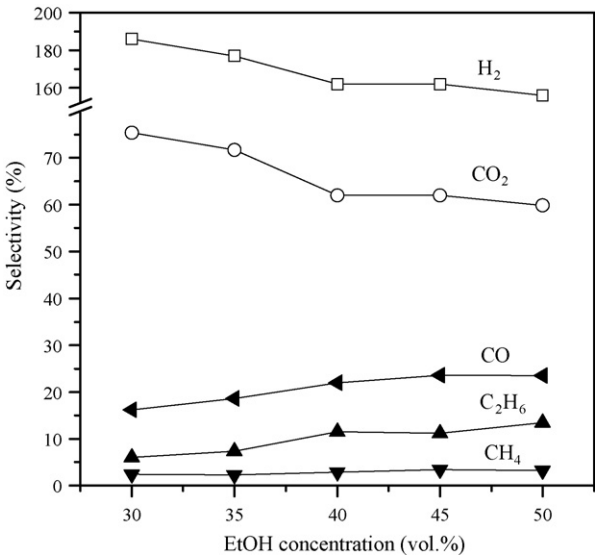

Fig. 4. Effect of EtOH volume concentration on selectivities to gas phase products of plasma-catalytic EtOH conversion using Pt/TiO_2 as WGS catalyst. Reaction conditions: 30–50 vol% EtOH, 0.1 mL/min, catalyst bed zone insulated, 1 g catalyst.

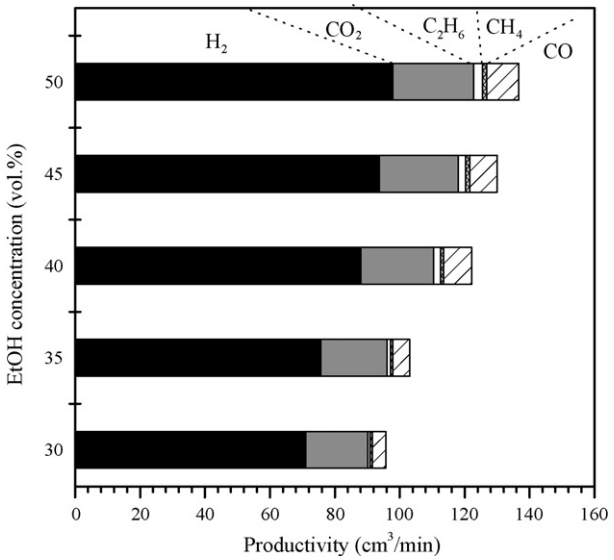

Fig. 5. Effect of EtOH volume concentration on gas phase products productivity of plasma-catalytic EtOH conversion using Pt/TiO_2 as WGS catalyst. Reaction conditions: 30–50 vol% EtOH, 0.1 mL/min, catalyst bed zone insulated, 1 g catalyst.

simulated post-plasma reaction (feed: 70% H_2–30% CO, no hydrocarbons) over the WGS catalysts used in this work, the hydrocarbons may be formed over the catalyst bed under the influence of the plasma by residual reactive species, since the catalyst and plasma are only separated by the macropores of the filter cap cathode electrode and some activated species may reach the catalyst through the macropores. These activated species could react on the catalyst to form additional CH_4 and C_2H_6. Another possibility for the additional hydrocarbons could be EtOH dehydration to C_2H_4 followed by hydrogenation to C_2H_6, and decomposition to CH_4 over the catalyst. The amount of hydrocarbons formed is dependent on the type of catalyst used.

When Pt/CeO_2 was used as the WGS catalyst with insulation, as shown in Fig. 3, it is seen that it has a higher CO_2 selectivity (79.7%) and lower CO selectivity (7.7%) than Pt/TiO_2 with insulation. The results are in agreement with the simulated post-plasma product (70% H_2–30% CO) test [28]. However, H_2 selectivity is slightly lower for Pt/CeO_2 (169.1%) than for Pt/TiO_2 (177.9%). This is because Pt/CeO_2 (4.5%) has a higher CH_4 selectivity than Pt/TiO_2 (2.3%) following the plasma. Methane formation consumes H_2, thus lowering the overall H_2 selectivity. Considering ceria is more expensive than TiO_2, and CH_4 favors formation over Pt/CeO_2, further study was focused on the TiO_2 supported catalysts.

Fig. 4 shows the effect of EtOH volume concentration on gas phase product selectivities using the Pt/TiO_2 catalyst for combined plasma reforming and catalytic WGS reaction. Increasing the EtOH concentration from 30% to 50% decreases the H_2 (186.1–156.0%) and CO_2 (75.4–59.8%) selectivities, but increases the C_2H_6 (6.0–13.5%), CH_4 (2.4–3.2%), and CO (16.2–32.5%) selectivities. This is as a result of less EtOH reforming and WGS reaction inhibition (equilibrium limitation due to composition) due to a decrease of the H_2O/EtOH and H_2O/CO ratios. However, increasing EtOH concentration increases the total H_2 productivity (from 71 to 98 cm^3/min) as well as CO_2, CO, CH_4, C_2H_6 productivity, as shown in Fig. 5. The CO composition increases from 4.1% to 7.0% with feed EtOH increasing from 30% to 50%. These results suggest that higher EtOH concentration favors higher productivity, whereas it also gives higher concentrations of undesirable products (for fuel cell applications, but not for H_2 enhanced combustion applications). 35% EtOH was selected for further study because it has a lower hydrocarbon selectivity and moderate H_2O/EtOH ratio.

Re promoted Pt/TiO_2 has been shown to be an active and stable catalyst for the WGS reaction [28,31]. 0.6 g $Pt–Re/TiO_2$ was used as a WGS catalyst for EtOH plasma reforming–catalytic WGS reaction (GHSV of ~10,000 $cm^3\,g^{-1}\,h^{-1}$), with results shown in Fig. 6. The experiment was carried out over 4 days with daily startup–shutdown (total time on stream of 26 h). The catalyst was directly exposed to the atmosphere without special protection when the reaction was shutdown. Both plasma and catalyst are found to be stable during the 4 days run. The EtOH conversion is higher than 90%. The H_2 concentration is around 73% throughout the 4 days run, which is very near to the nominal H_2 concentration (75%) if the reaction follows reaction (3). The CO_2 concentration is about 21% and the C_2H_6 and CH_4 concentrations are maintained at about 1.2% and 1%, respectively. Also, the hydrocarbon concentrations are lower than reported in the literature [4,6,18]. The CO concentration is about

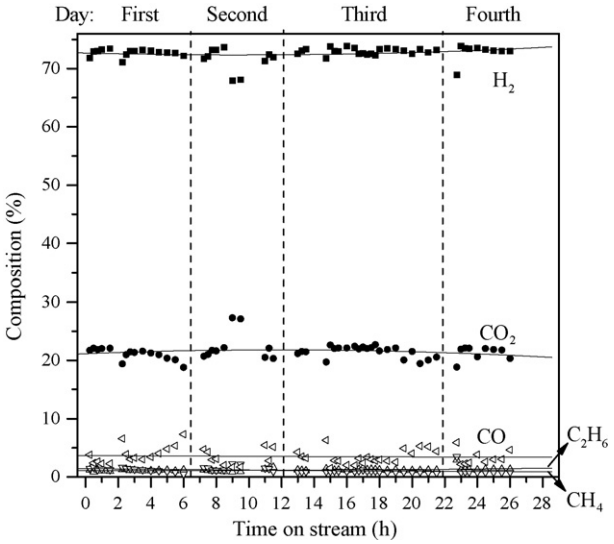

Fig. 6. Effect of time on stream and daily startup–shutdown cycles on gas phase compositions using $Pt–Re/TiO_2$ as WGS catalyst of plasma-catalytic ethanol conversion. Reaction conditions: 35 vol% EtOH, 0.1 mL/min, catalyst bed zone insulated, 0.6 g catalyst.

3.8% during the 4 days run, which is lower than with the Pt/TiO_2 catalyst with a GHSV of 6000 $cm^3\,g^{-1}\,h^{-1}$. Usually, the CO concentration was a little higher when the reaction was first started up. A comparison with the Pt/TiO_2 results shows that the $Pt–Re/TiO_2$ is initially more active for CO conversion, although it promotes CH_4 a little, as shown in Table 2.

Considering the fact that (a) $Pt–Re/TiO_2$ is more active for WGS but increases CH_4 formation (methanation) under the plasma influence; (b) Pt/TiO_2 is a little less active for the WGS reaction but also less active for methanation and (c) the temperature of the catalyst zone in contact with the plasma is higher, near where the WGS reaction is expected to approach thermodynamic equilibrium, but methanation will be decreased due to the higher temperature. We therefore used a double catalyst bed, with the Pt/TiO_2 (0.4 g) as the first catalyst bed, which is in direct contact with the plasma, and $Pt–Re/TiO_2$ (0.6 g) as a second catalyst bed (GHSV is ~6000 $cm^3\,g^{-1}\,h^{-1}$). In this configuration, the WGS should approach equilibrium in the first bed with methanation small due to Pt/TiO_2 being less active for methanation. Then, in the second bed, the residual CO will be further converted to CO_2 and H_2 with methanation activity also quite low due to the lower temperature. The results of the Pt/TiO_2 and $Pt–Re/TiO_2$ stacked bed configuration are summarized in Table 2. The EtOH conversion to gas phase products is higher than 90% during the 300 min run, which is similar to the previous single WGS catalyst bed results. The gas phase composition is also stable for plasma ethanol reforming with the stacked catalyst bed. H_2 (~73%) and CO_2 (~23%) are the main gas phase products. C_2H_6 and CH_4 are the hydrocarbon products, with concentration of about 1.4% and 0.9%, respectively and the desired reduction of methanation activity was achieved. Compared with the $Pt–Re/TiO_2$ (0.6 g) one bed reactor, the stacked bed reactor reduced CO concentration significantly from 3.8% to 0.8%. This concentration of CO in the product gas is sufficiently low to be directly processed with CO preferential oxidation to remove the residual CO. The H_2 concentration in this study is among the highest reported in the literature using a single reactor [35] or a reaction system [11,36]. Most importantly, no diluents were used and the GHSV is higher in this study.

Fig. 7 shows the effect of feed flow rate on the gas phase productivity and EtOH conversion using the stacked bed. It can be seen that an increase of feed flow rate from 0.1 to 0.23 ml/min increases the total productivity gradually from 105 to 201 cm^3/min.

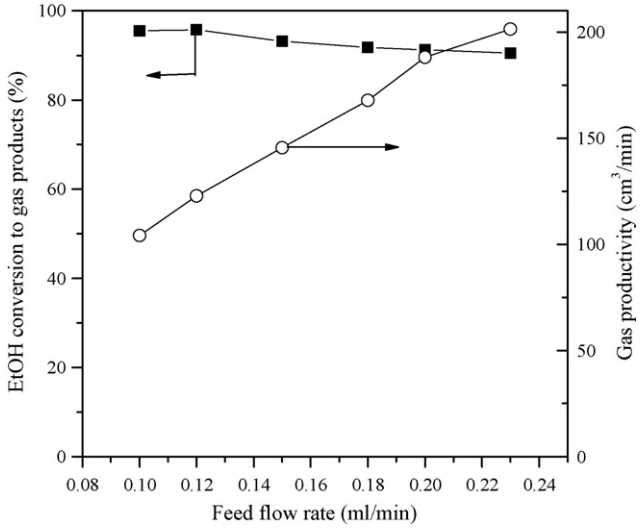

Fig. 7. Effect of feed flow rate on EtOH conversion and gas phase productivity using stacked bed WGS catalyst of plasma-catalytic EtOH conversion. Reaction conditions: 35 vol% EtOH, catalyst bed zone insulated, 0.4 g Pt/TiO_2 followed by 0.6 g $Pt–Re/TiO_2$.

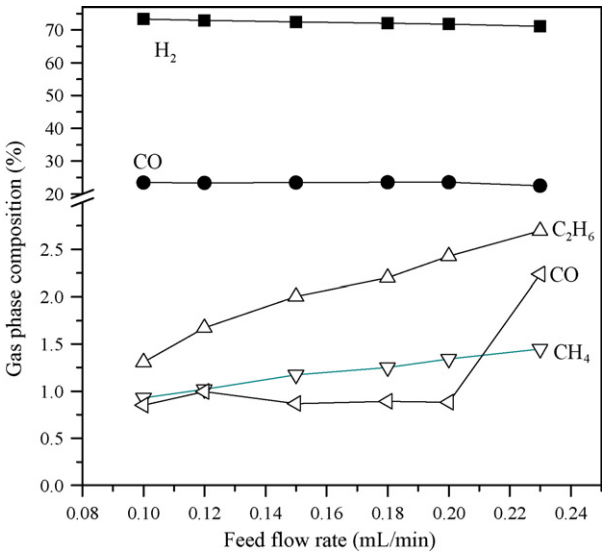

Fig. 8. Effect of feed flow rate on gas phase composition using stacked bed WGS catalyst of plasma-catalytic EtOH conversion. Reaction conditions: 35 vol% EtOH, catalyst bed zone insulated, 0.4 g Pt/TiO_2 followed by 0.6 g $Pt–Re/TiO_2$.

Whereas the EtOH conversion to gas phase products decreases from 95% to 90%. Fig. 8 shows the gas phase composition changes vs feed flow rate. The H_2 and CO_2 compositions only slightly decrease, about 2% and 1%, respectively, with increasing feed flow rate from 0.1 to 0.23 ml/min. C_2H_6 and CH_4 compositions gradually increase from 1.3% and 0.9% to 2.7% and 1.5%, respectively. CO concentration remain about 0.8% for feed flow rates lower than 0.2 ml/min, but increases to 2.2% when the flow rate increases up to 0.23 ml/min. These results imply that the WGS reaction can be operated up to 0.2 ml/min feed flow rate, i.e. GHSV of ~12,000 $cm^3\,g^{-1}\,h^{-1}$, with an acceptable CO concentration.

Figs. 9 and 10 show the effect of time on stream on the EtOH conversion and gas phase composition for the conditions of 0.15 ml/min feed flow rate (GHSV is ~9000 $cm^3 g^{-1} h^{-1}$) of 35% EtOH. It can be seen that both the EtOH conversion and the gas phase compositions are very stable over the tested time on stream. The CO concentration remains lower than 1%.

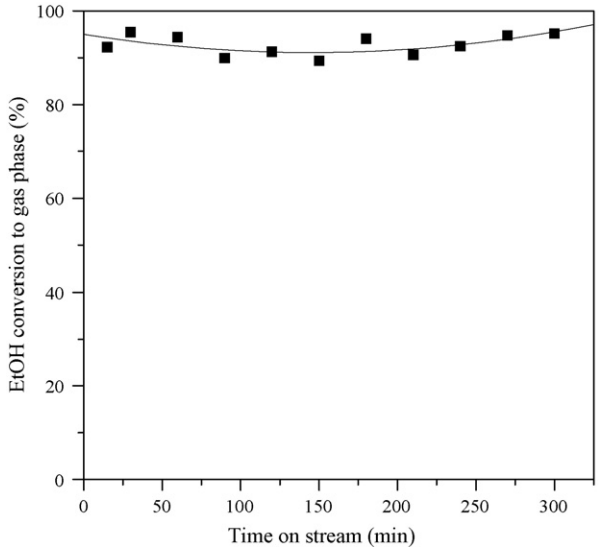

Fig. 9. Effect of time on stream on EtOH conversion using stacked bed WGS catalyst of plasma-catalytic EtOH conversion.

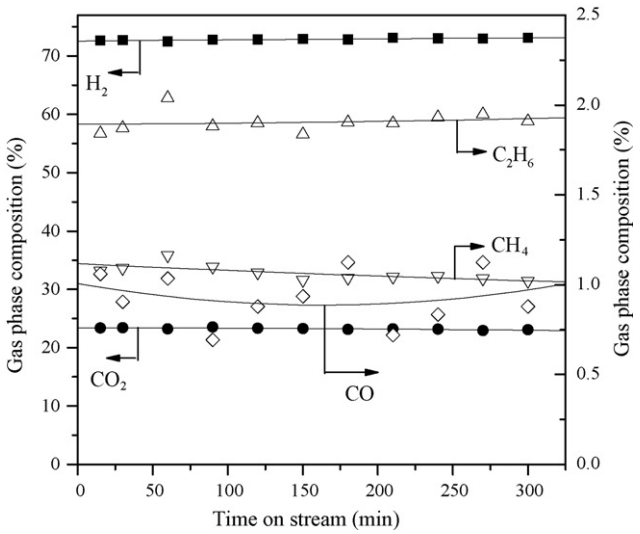

Fig. 10. Effect of time on stream on gas phase composition using stacked bed WGS catalyst of plasma-catalytic EtOH conversion.

There is a little coke formed on the walls of the reactor as well as on the sides of the electrodes, where the plasma is extinguished due to re-combination of the active species (electrons, radicals, ions) by collisions with the surfaces. However, the tip of the anode and the top of the cathode between where the plasma is formed remain clean. Therefore, the coke formation has no influence on the catalyst bed that is located under the cathode electrode and inside 3/8 in. tube. Furthermore, it should be noted that the plasma is stable up to 95% EtOH (H_2O/EtOH = 0.17). EtOH concentrations higher than 95% reduce the stability of the plasma over time due to the accumulation of carbon deposits, as is the case with all reforming reaction systems.

Using the plasma-catalytic reactor with a proper catalyst, the overall reaction of bio-ethanol reforming follows closely to the ideal reaction (3), resulting in product gases containing ~73% H_2 and ~23% CO_2, with small amounts of CO (~0.8%), CH_4, and C_2H_6. Since both CH_4 and C_2H_6 are inert for the Pt electrode of fuel cell, the resultant gases can be directly processed by CO preferential oxidation for H_2 fuel cell application. The reactor is also compact because no diluent gases are used and no external heating is needed. With an acceptable CO concentration, the space velocity for WGS could be as high as ~12,000 $cm^3\ g^{-1}\ h^{-1}$, which may be improved with further catalyst development, for example, Na promoted Pt/TiO_2 [28]. The plasma-catalytic system has the advantages of the plasma reaction, i.e. relatively low temperature, fast response, free of catalyst deactivation due to coke formation, and good efficiency. Therefore, the plasma-catalytic reactor may be a good candidate for smaller scale H_2 production for fuel cell applications of H_2 enhanced combustion. It may also be extended to other applications, where the plasma initiates reactions and a catalyst selectively enhances the desirable reaction.

4. Conclusions

Bio-ethanol reforming was studied using a plasma-catalytic reactor for H_2 production. The feed was fed through the anode and the WGS catalyst was put just below the cathode. Thus the heat produced from the plasma was effectively used in feed gasification and WGS reaction. The combined plasma reforming and catalytic WGS using this reactor make the overall reaction follow ethanol reforming to H_2 and CO_2, with small amounts of CO, CH_4 and C_2H_6. When Pt/TiO_2 and $Pt–Re/TiO_2$ are used as stacked bed WGS catalysts, the CO concentration could be lowered to ~0.8% with a gas hourly space velocity up to 12,000 $cm^3\ g^{-1}\ h^{-1}$. Stability tests with daily startup–shutdown showed both plasma and catalyst are quite stable up to 26 h. The plasma-catalytic reactor combines the advantages of both plasma reaction and catalytic reaction.

Acknowledgment

The support from SEMGREEN LP is greatly appreciated.

References

[1] J.R. Rostrup-Nielsen, Phys. Chem. Chem. Phys. 3 (2001) 283.
[2] G.W. Huber, J.W. Shabaker, J.A. Dumesic, Science 300 (2003) 2075.
[3] G.A. Deluga, J.R. Salge, L.D. Schmidt, X.E. Verykios, Science 303 (2004) 993.
[4] F. Aupretre, C. Descorme, D. Duprez, D. Casanave, D. Uzio, J. Catal. 233 (2005) 464.
[5] A.N. Fatsikostas, X.E. Verykios, J. Catal. 225 (2004) 439.
[6] T. Montini, L.D. Rogatis, V. Gombac, P. Fornasiero, M. Graziani, Appl. Catal. B 71 (2007) 125.
[7] T. Bunluesin, R.J. Gorte, G.W. Graham, Appl. Catal. B 15 (1998) 107.
[8] Y. Li, Q. Fu, M. Flytzani-Stephanopoulos, Appl. Catal. B 27 (2000) 179.
[9] J.M. Zalc, D.G. Löffler, J. Power Sources 111 (2002) 58.
[10] D. Sopeña, A. Melgar, Y. Briceño, R.M. Navarro, M.C. Álvarez-Galván, F. Rosa, Int. J. Hydrogen Energy 32 (2007) 1429.
[11] M. Benito, R. Padilla, J.L. Sanz, L. Daza, J. Power Sources 169 (2007) 123.
[12] B. Eliasson, U. Kogelschatz, IEEE Trans. Plasma Sci. 19 (1991) 1063.
[13] C.J. Liu, G.H. Xu, T.M. Wang, Fuel Process. Technol. 58 (1999) 119.
[14] G. Petitpas, J.D. Rollier, A. Darmon, J. Gonzalez-Aguilar, R. Metkemeijer, L. Fulcheri, Int. J. Hydrogen Energy 32 (2007) 2848, and references therein.
[15] M.G. Sobacchi, A.V. Saveliev, A.A. Fridman, L.A. Kennedy, S. Ahmed, T. Kraus, Int. J. Hydrogen Energy 27 (2002) 635.
[16] S.L. Yao, A. Nakayama, E. Suzuki, AIChE J. 47 (2001) 419.
[17] Y. Sekine, K. Urasaki, S. Kado, M. Matsukata, E. Kikuchi, Energy Fuels 18 (2004) 455.
[18] A. Yanguas-Gil, J.L. Hueso, J. Cotrino, A. Caballero, A.R. González-Elipe, Appl. Phys. Lett. 85 (2004) 4004.
[19] O. Aubry, C. Met, A. Khacef, J.M. Cormier, Chem. Eng. J. 106 (2005) 241.
[20] J.J. Zou, C.J. Liu, Y.P. Zhang, Energy Fuel. 20 (2006) 1674.
[21] L. Bromberg, D.R. Cohn, A. Rabinovich, N. Alexeev, A. Samokhin, K. Hadidi, J. Palaia, N. Margarit-Bel, PSFC JA-06-3 (2006) 1.
[23] H.L. Chen, H.M. Lee, S.H. Chen, Y. Chao, M.B. Chang, Appl. Catal. B 85 (2008) 1, and references therein.
[24] K. Supat, S. Chavadej, L.L. Lobban, R.G. Mallinson, Ind. Eng. Chem. Res. 42 (2003) 1654.
[25] C.L. Gordon, L.L. Lobban, R.G. Mallinson, Catal. Today 84 (2003) 51.
[26] X.L. Zhu, T. Hoang, L.L. Lobban, R.G. Mallinson, Chem. Commun. (2009) 2908.
[27] H. Le, L.L. Lobban, R.G. Mallinson, Catal. Today 89 (2004) 15.
[28] X.L. Zhu, T. Hoang, L.L. Lobban, R.G. Mallinson, Catal. Lett. 129 (2009) 135.
[29] G. Jacobs, R.A. Keogh, B.H. Davis, J. Catal. 245 (2007) 326.
[30] P. Panagiotopoulou, A. Christodoulakis, A.I. Kondarides, S. Boghosian, J. Catal. 240 (2006) 114.
[31] K.G. Azzam, I.V. Babich, K. Seshan, L. Lefferts, J. Catal. 251 (2007) 163.
[32] T. Hoang, L.L. Lobban, R.G. Mallinson, In preparation.
[33] B.E. Spiewak, R.D. Cortright, J.A. Dumesic, J. Catal. 176 (1998) 405.
[34] C.K. Shi, R. Hoisington, B.W.L. Jang, Ind. Eng. Chem. Res. 46 (2007) 4390.
[35] N. Homs, J. Llorca, P.R.D.L. Piscina, Catal. Today 116 (2006) 361.
[36] A.M. Silva, A.M.D.D. Farias, L.O.O. Costa, A.P.M.G. Barandas, L.V. Mattos, M.A. Fraga, F.B. Noronha, Appl. Catal. A 334 (2008) 179.